Folz, S. D.; Kratzer, D. D.; Kakuk, T. J.; Rector, D. L. *J. Vet. Pharmacol. Ther.* **1984**, *7*, 29.
Geissbuhler, H.; Kossmann, K.; Baunok, I.; Boyd, V. F. *J. Agric. Food Chem.* **1971**, *19*, 365.
Giles, D. P.; Kerry, J. C.; Rothwell, D. N. *Proc. Br. Crop Prot. Conf.* **1979**, 265.
Harrison, I. R.; Kozlik, A.; McCarthy, J. F.; Palmer, B. H.; Wakerley, S. B.; Watkins, T. I.; Weighton, D. M. *Pestic. Sci.* **1972**, *3*, 679.
Hornish, R. E., The Upjohn Co., Kalamazoo, MI, unpublished data, 1983.
IUPAC, Chemical Division. *Spectrochim. Acta, Part B* **1978**, *33B*, 247.
Knowles, C. O.; Benezet, H. J. *J. Environ. Sci. Health, Part B* **1981**, *B16* (5), 547.
Knowles, C. O.; Gayen, A. K. *J. Econ. Entomol.* **1983**, *76*, 410.
Knowles, C. O.; Roulston, W. J. *J. Econ. Entomol.* **1973**, *66*, 1245.
Leeper, J. R.; Reissig, W. H. *J. Econ. Entomol.* **1980**, *73*, 104.
Lewis, D. K., The Boots Co., Nottingham, U.K., unpublished data, 1972.
Long, G. L.; Weinfordner, J. D. *Anal. Chem.* **1983**, *55*, 713A.
MacDougall, D.; Crummett, W. B. *Anal. Chem.* **1980**, *52*, 2242.
Shirk, M. E. *VM/SAC, Vet. Med. Small Anim. Clin.* **1983**, *78*, 1059.
Somerville, L. "Program and Abstracts", First International Symposium of Foreign Compound Metabolism, West Palm Beach, FL, Oct 1983; International Society for the Study of Xenobiotics: Robbinsville, NJ, 1983.
Somerville, L.; Nickelson, J. E., The Boots Co., Nottingham, U.K., unpublished data, 1972.
Staten, F. W.; Thornton, A. W., The Upjohn Co., Kalamazoo, MI, unpublished results, 1975.
Staten, F. W.; Thornton, A. W.; Cox, B. L.; VanDerSlik, A. L., The Upjohn Co., Kalamazoo, MI, unpublished results, 1973.
Weighton, D. M.; Osborne, W. B. *Proc. Br. Insectic. Fungic. Conf.* **1973**, *7*, 309.

Received for review March 5, 1984. Revised manuscript received July 16, 1984. Accepted August 14, 1984.

Kinetics and Mechanism of Alkaline and Acidic Hydrolysis of Aldicarb

Shelton Bank* and R. Jeffrey Tyrrell

The hydrolysis of aldicarb, 2-methyl-2-(methylthio)propanal *O*-[(methylamino)carbonyl]oxime, was investigated over the pD (pH) region 3.0–8.6 by using pulse Fourier transform nuclear magnetic resonance (FT NMR). At pH values above 7.0, a base-catalyzed carbamate decomposition via methyl isocyanate is observed. The principal products are the oxime of 2-methyl-2(methylthio)propanol, dimethylurea, methylamine, and carbon dioxide. At pH values below 5.0 an unusual acid-catalyzed reaction leading principally to 2-methyl-2(methylthio)propionitrile and methylamine was found. In the intervening and environmentally significant acidity regions, both schemes were obtained. Minor products in both reactions include those from the small amount of anti isomer as well as other reaction paths for the syn isomer. These results indicate that at the pH and temperature of the Long Island aquifer aldicarb is likely to remain a contaminant for many years.

Recently, aldicarb, 2-methyl-2-(methylthio)propanal *O*-[(methylamino)carbonyl)]oxime (I), has been found

$$CH_3SC(CH_3)_2CH{=}NOC(O)NHCH_3$$

I

contaminating the aquifers in New York (Guerrera, 1981). The contamination was initially considered unique to the Long Island geography. However, other areas of the country, such as Arizona, Maine, Virginia, and Wisconsin, have also experienced groundwater contamination from aldicarb (Cohen et al., 1984). A most recent occurrence has been in Florida where the pesticide was used to control orange crop pests (Cohen et al., 1984).

Since introduction in 1965 (Weiden et al., 1965), this carbamate pesticide has been widely used for protection of commercial crops, such as cotton, potatoes, peanuts, sugar beets, corn, sweet potatoes, and many others, from attack by mites, nematodes, and other pests (Richey et al., 1977). Aldicarb has a high degree of contact toxicity to a variety of insects and a remarkable systemic potency. Most conveniently, it is planted with the crops in the spring and absorbed into the plants as they grow, thus providing nearly seasonal protection from these insects.

Many laboratory and field studies have been performed to determine aldicarb degradation in soils and crops, and these are valuably summarized (Maitlen and Powell, 1982). Of primary interest to this work, the pathways involve oxidation to aldicarb sulfoxide and sulfone and hydrolysis to aldicarb oxime, aldicarb sulfoxide oxime, and aldicarb sulfane oxime. These pathways are apparently less important in some soils. When aldicarb was used on Long Island, NY, where the water table is high, the pesticide was found to make a rapid migration into the Upper Glacial Aquifer (Guerrera, 1981).

This discovery of aquifer contamination by aldicarb, which led to a ban on its usage on Long Island, underscores the need to learn the fate of this pesticide after it has entered the underground waters. Once in the aquifer some of the degradative pathways available in surface soils, such as photolysis by sunlight, are no longer available, and some such as biolysis by soil microbes are less likely. The major degradative process remaining is hydrolysis and is likely without oxidative pathways. In actual fact, whereas aldicarb is rapidly oxidized in many environments (Maitlen and Powell, 1982), analyses of some Long Island well waters show predominance of the unoxidized sulfide form (Eadon, 1984).

In the Long Island aquifer this must take place at a pH of approximately 5.5 and a temperature of about 11 °C. Even for chemicals as widely used as aldicarb, little has been reported about its fate and persistence in natural water systems. Long-term hydrolysis of aldicarb leads to significant decay at pH 8.5 and 15 °C in 186 days (Hansen

Department of Chemistry, State University of New York at Albany, Albany, New York 12222.

0021-8561/84/1432-1223$01.50/0

and Spiegel, 1983). The lack of information concerning carbamate hydrolysis under varying conditions prompted our research efforts to determine the rate, mechanism, and product composition of aldicarb hydrolysis.

FT NMR spectroscopy was chosen to follow the course of this reaction because of the difficulties involved in using more conventional kinetic techniques, such as ultraviolet spectroscopy (UV), gas–liquid chromatography (GLC), or high-performance liquid chromatography (HPLC). In recent years, NMR spectroscopy has been employed frequently for kinetic analysis of hydrolytic reactions (Macomber, 1983; Okuyama and Fueno, 1983). FT NMR was selected for following aldicarb (I) hydrolysis and found to provide the most efficient and simple method of determining the concentrations of the reactants and products throughout the reaction. Fourier transform techniques provided the high signal to noise ratio necessary for accurate analysis due to the necessarily low concentrations of products and reactants used in the reaction. Additionally, the digital analyzer interfaced to the spectrometer provided accurate determination of integration and intensity values of the reactants that were used to follow the kinetics of hydrolysis.

MATERIALS AND METHODS

Proton NMR spectra (60 MHz) were obtained by using a Varian EM-360A nuclear magnetic resonance spectrometer. ^1H NMR spectra (90-MHz) and ^{13}C NMR spectra (22.64 MHz) were obtained on a Bruker WH-90 spectrometer equipped with a Bruker B-NC-12 data collection system interfaced to a Nicolet Model 294 disc drive. The spectra were run in the Fourier transform mode by using quadrature detection and a standard-phase alternated pulse sequence (PAPS). ^{13}C NMR spectra were run with both broad-band and off-resonance decoupling. A spectral width of 5500 Hz was used with digitization over 8K data points. Exponential line broadening of 1 Hz was used in all cases. Chemical shifts for ^1H and ^{13}C spectra are reported on the δ scale downfield from tetramethylsilane (Me_4Si; TMS in the figures) for spectra taken in organic solvents or downfield from 3-(trimethylsilyl)-1-propanesulfonic acid (DSS) for samples taken in D_2O.

Mass spectral data were collected on an AEI MS-902 high-resolution electron impact mass spectrometer. Gas–liquid chromatographic analyses (GLC) were performed on a Hewlett-Packard Model 5750 research chromatograph. A 5 ft × $^1/_8$ in. stainless steel column, packed with 30% SE-30 on Chrom W, 60–80 mesh, was routinely used for analysis. Ultraviolet (UV) spectra were run on a Varian DMS 90 UV–vis spectrophotometer. Melting points were determined on a Mel-Temp apparatus (capillary method) and are uncorrected. pH measurements were made with an Altex ϕ 30 digital p*H* meter equipped with a gel electrode.

Commercially available reagents were used whenever possible. Solvents were Fisher reagent grade and used without further purification. Buffer components were also Fisher reagent grade. A 25-L Tamson (Holland) oil bath and circulator were used to control temperatures to ±0.1 °C for the NMR kinetic studies. The oil and water baths used for the GLC and UV–vis kinetic studies were temperature controlled and monitored with either an I^2R Model L7-1100B Therm-O-Watch or a Sargant Thermonitor.

Chemicals. The preparation of 2-methyl-2-(methylthio)propanal *O*-[(methylamino)carbonyl]oxime (I) followed literatures procedures with some modifications (Payne et. al., 1966). The preparation starts from 2-methylpropene, which was prepared by reaction of sodium ethoxide (Fieser and Fieser, 1967) and 2-chloro-2-methylpropane (Eastman). The 2-methylpropene nitrosochloride dimer was prepared by the method of Meinwald et al. (1964) from 2-methylpropene and 2-nitritopentane (Pfaltz and Bauer). The preparation yielded 31 g (0.14 mol) of nitrosochloride dimer: 32%; mp 99–100 °C; ^1H NMR δ 1.76 (s, 6 H), 4.71 (s, 2 H), 7.39 (br s, 1 H).

Methanethiol was prepared by reduction of methyl disulfide (Emerson, 1951). 2-Methyl-2-(methylthio)propanal oxime (II) was prepared by the method of Payne et al. (1966) from methanethiol and 2-methylpropene nitrosochloride dimer, which afforded 24.3 g (0.18 mol, 73%) of a light yellow oil: bp 90–92 °C/10 mmHg; lit. bp 82–93 °C/8 mmHg (Payne et al., 1966); ^1H NMR (EM-360A neat) δ 1.39 (s, 6 H), 1.93 (s, 3 H), 7.30 (s, 1 H), 9.06 (br s, 1 H); IR (C=O) 1720, (C—O) 1240, (NH) 3350, 1510 cm^{-1} (Payne et al., 1966).

2-Methyl-2-(methylthio)propanol *O*-[(methylamino)-carbonyl]oxime (I) was then prepared following the reported procedure (Payne et al., 1966), in which 2-methyl-2-(methylthio)propanal oxime (II) was reacted with an excess of methyl isocyanate (Aldrich). There was obtained 18.5 g (0.097 mol, 88.4%) of long white needle crystals: mp 99–101 °C; lit. mp 99–100 °C (Payne et al., 1966); ^1H NMR (EM-360A $CDCl_3$) δ 1.45 (s, 6 H), 1.97 (s, 3 H), 2.93 (d, 3 H), 6.1 (br s, 1 H), 7.54 (s) plus 7.34 (small s), which combined integrate for 1 H.

2-Methyl-2-(methylthio)propionitrile (III). The nitrile (II) was prepared via thermal decomposition (200 °C) of I with the rapid evolution of carbon dioxide gas. The resulting oil residue was distilled to afford 3.2 mL (0.025 mol) of 2-methyl-2-(methylthio)propionitrile (III); bp 61 °C/20 mmHg; lit. bp 73 °C/40 mmHg (Payne et al., 1966); ^1H NMR ($CDCl_3$) δ 1.6 (s, 6 H), 2.24 (s, 3 H); IR (neat) (C=N) 2226, [$(CH_3)_2C$] 1387.7, 1368.7, (CH_3–S) 1321.3 cm^{-1}; mass spectrum *m/e* 115.

1,3-Dimethylurea. A solution of 0.3 g (5.3 mmol) of methyl isocyanate in 20 mL of water (pH 8.0) was stirred at room temperature for 90 min. The solvent was removed in vacuo to afford white crystals: mp 99–101 °C; ^1H NMR (D_2O/DSS) δ 2.6 (s, 6 H); IR (Nujol mull) 3300 (br s), 1600 (s), 1580, 1460 cm^{-1}.

2-Methyl-2-(methylthio)propanal (IV). I (0.5 g, 0.004 mol) was dissolved in 20 mL of aqueous solution of hydrochloric acid (pH 0.0) and heated with stirring for 20 h at 70 °C. The cooled solution was extracted with ether (3 × 25 mL) and the ether extracts were dried over sodium sulfate. The ether was evaporated to afford an oil. Analysis of this resulting oil (IR and NMR) revealed it to be a mixture of oxime (II) and aldehyde (IV) in approximately a 40:60 ratio: ^1H NMR (EM-360A, $DCDl_3$) δ 1.37 ppm (s, 6 H, aldehyde IV), 1.4 (s, 6 H, oxime II), 1.7 ppm (s, 3 H, aldehyde IV), 1.93 ppm (s, 3 H, oxime II), 7.18 (s, 1 H, oxime II), 8.93 ppm (s, 1 H, aldehyde IV); IR [C(O)–H (aldehyde)] 2830, 2780, (oxime C–H) 2725, (oxime NOH) 3310 cm^{-1}.

Kinetic Methods. Buffers used in the kinetic studies were prepared according to the methods described by Gomori (1955). Reagent-grade buffer components and distilled water were used throughout. Stock solutions were prepared and appropriately mixed to obtain the desired pH values. The ionic strength of the solutions was kept constant at 0.7 with potassium chloride.

Deuterated Buffers. A 25-mL Pyrex vacuum flask was charged with 10.0 mL of appropriate buffer, which was frozen in a "shell" around the wall of the flask. The frozen sample was immediately placed on the Virtis lyophilizer and evacuated. Lyophilization (–55 °C/0.02 mmHg) was

Table I. Sample Calculation of Pseudo-First-Order Rate Constants from NMR Spectral Data[a,b]

time min	intensity value DSS	intensity value aldicarb	relative concn	% residual aldicarb	ln (% residual aldicarb)
0	0.511	2.178	426	100	4.605
10	0.540	1.813	336	79	4.37
20	3.635	8.548	235	55	4.01
30	3.586	6.289	175	41	3.72
43	0.429	0.514	120	28	3.34
60	1.868	1.476	79	19	2.92
70	3.820	2.567	67	16	2.76

[a] For these data a pseudo-first-order rate constant of $k_1 = 4.54 \times 10^{-4}$ s^{-1} with a correlation coefficient (r) = 0.996 is obtained. [b] At 90 °C and pD 7.53 with deuterated phosphate buffer, 0.05 M. Ionic strength raised to 0.70 with potassium chloride. Initial aldicarb concentration 0.0087 M.

complete in 4–6 h. The powder is reconstituted by adding 10.0 mL of deuterium oxide (99.9% D S.I.C.) to the vacuum flask. The deuterated buffer is stored in a bottle under nitrogen and sealed with parafilm. pD measurements were obtained by placing 1 mL of the buffer in a 15-cm test tube. The gel electrode was inserted into the test tube and the reading taken from the pH meter. The proper pD value was obtained by adding 0.4 pH unit to the observed meter reading (Bender and Homer, 1965; Glasoe and Long, 1960). The pD of the buffers was not adjusted.

Nuclear Magnetic Resonance Spectroscopic Technique. Standard solutions (0.0087 M) were prepared by dissolving 4 mg (0.02 mmol) of aldicarb (I) in 2.4 mL (1.66 mg/mL) of deuterated buffer for the pH values to be studied. ^{1}H NMR samples were prepared in 5-mm proton tubes with 0.5 mL of deuterated carbamate standard and one crystal of 3-(trimethylsilyl)-1-propanesulfonic acid (DSS, Aldrich). The proton tubes were flushed with argon, capped, and, in select instances, sealed with parafilm. For each kinetic run the samples were prepared in duplicate and analyzed simultaneously. The tubes were heated in a 25-L P. T. Tamson oil bath, which maintained the temperature to ±0.1 °C.

An initial spectrum was taken for each of the samples prior to hydrolysis in order to obtain the initial concentration of aldicarb (I). At appropriate times, duplicate tubes were withdrawn from the oil bath and the reaction was quenched by immersion in a large ice–water bath. Since negligible hydrolysis occurs at room temperature, the reaction tubes were allowed to warm to room temperature for analysis.

FT NMR spectra (90 MHz) were taken of each sample to determine the extent of hydrolysis and the identity of the products. The concentrations of aldicarb (I) remaining and of products formed during the reaction were calculated by comparing the integration values of these compounds with the integration value of the DSS standard at each time interval. The rate of hydrolysis was calculated by following the depletion of aldicarb (I) as the reaction progressed. The rate constants were obtained from the intensity value for aldicarb (I) (obtained from the digital analyzer) divided by the intensity value for DSS at each time to yield a relative concentration value. The slope of the linear regression analysis of ln percent residual aldicarb (I) vs. time affords the pseudo-first-order rate constant (Table I).

RESULTS AND DISCUSSION

The proton and ^{13}C spectra of aldicarb (I) and the expected alkaline hydrolysis product, aldicarb oxime (II) (Figures 1 and 2), consisted of well-separated singlets and

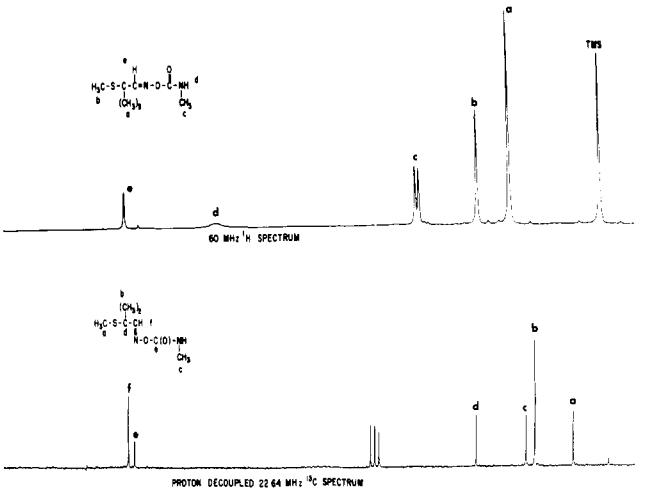

Figure 1. Proton and ^{13}C NMR spectra of aldicarb (I) [2-methyl-2-(methylthio)propanal *O*-[(methylamino)carbonyl]oxime] in deuteriochloroform. For the proton NMR the labeled assigned peaks (see structure) are as follows (in ppm): a, 1.45; b, 1.98; c, 2.93; d, 6.10; e, 7.54 and 7.34. For the ^{13}C NMR the labeled assigned peaks are as follows (in ppm): a, 11.56, b, 24.55; c, 27.54; d, 44.04; e, 155.84; f, 157.66.

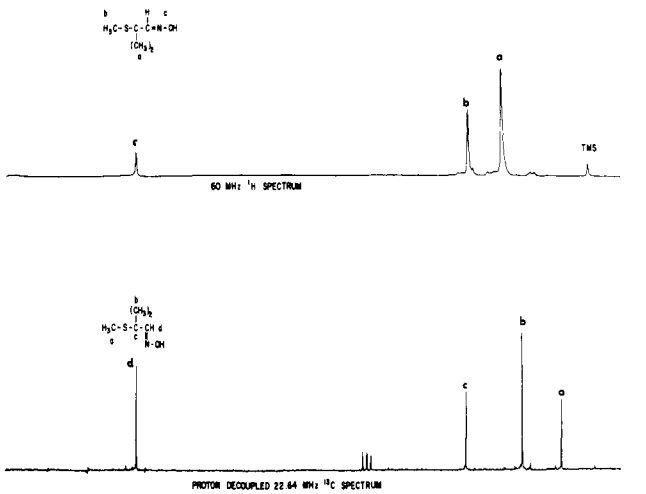

Figure 2. Proton and ^{13}C NMR spectra of aldicarb oxime (II) [2-methyl-2-(methylthio)propanal oxime]. For the proton NMR the labeled assigned peaks are as follows (in ppm): a, 1.39; b, 1.93; c, 7.30. For the ^{13}C NMR the labeled assigned peaks are as follows (in ppm): a, 11.25; b, 24.76; c, 44.12; d, 154.43.

were easily assigned by literature analogies. In Figure 1, the singlet at 7.53 ppm (e) and the small singlet at 7.34 ppm, which combined integrate for one proton, were assigned by Payne et al. (1966) and interpreted to indicate that aldicarb (I) exists in both syn and anti conformations. In the syn conformer the imine proton lies in a region that is more deshielded than it does in the anti isomer, and on this basis, the NMR spectrum indicates that aldicarb (I) exists primarily in the syn configuration (7.5 ppm, 96%) with minor amounts of the anti conformer (7.34 ppm, 4%). Additional evidence for this conformational assignment came from the reaction sequence developed by Hauser and Jordan (1935, 1936), who defined the syn isomer as the conformation with the imine proton and the oxime oxygen on the same side of the carbon–nitrogen double bond: i.e., "cis" to one another. These assignments for aldicarb oxime (Figure 2) were made on the basis of chemical shift data and published spectral data (Payne et al., 1966). Due to the simplicity of these spectra and the ease of identification of the signals for these compounds, straightforward kinetic

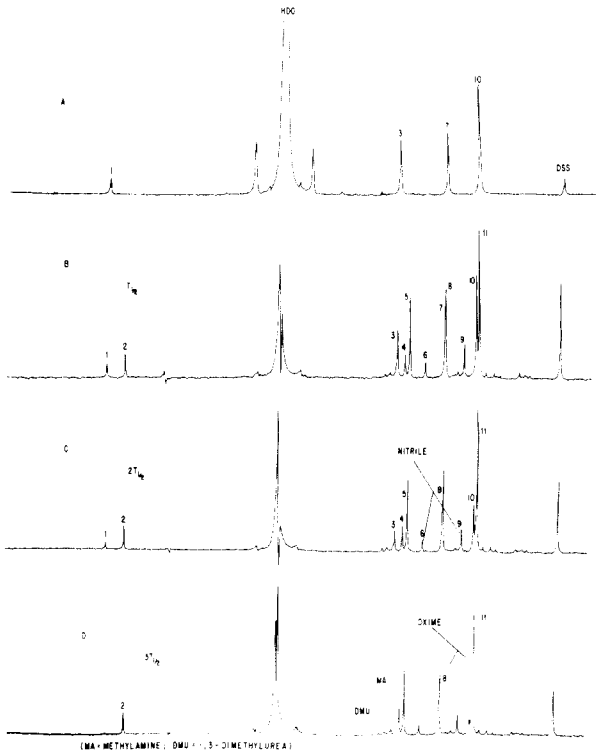

Figure 3. 90-MHz proton NMR spectra of aldicarb (I) hydrolysis in pD 7.53 phosphate buffer at 90 °C. (A) Initial reaction solution; (B) reaction solution at $\tau_{1/2}$; (C) reaction solution at $2\tau_{1/2}$; (D) reaction solution at $3\tau_{1/2}$.

analysis of alkaline hydrolysis was achieved by FT NMR spectroscopy. This is clearly demonstrated in the series of proton spectra presented in Figure 3.

As the hydrolysis reaction time increases (Figure 3), those signals ascribed to aldicarb (I) (Figure 3A) diminish in intensity and other signals ascribed to the products of the reaction appear. Figure 3B illustrates the more complex spectrum of the reaction mixture after slightly more than one half-life. This spectrum is composed of signals that have been assigned both to aldicarb (I) and those due to the resonances of the expected oxime (II) product. A particularly visible change in the initial spectrum involves the imine proton region of the spectra. The signal at 7.73 ppm (peak 1 in Figure 3A) has dimininshed in intensity and is replaced by a peak 0.3 ppm upfield at 7.42 ppm (peak 2 in Figure 3B), which is assigned to the aldoxime proton of the product. The change in chemical shift and intensity of these peaks can be used to monitor both the rate of hydrolysis of aldicarb (I) and the rate of formation of the oxime (II). The signal of the *gem*-dimethyl protons is also shifted upfield by 0.050 ppm from 1.456 ppm in aldicarb (I) (peak 10) to 1.405 ppm in the oxime product (II) (peak 11). This change can be used preferably to follow the rate of aldicarb (I) hydrolysis due to the ease and increased accuracy of measuring the six-proton signal. This was particularly useful during the later stages of the reaction where little change in intensity of product occurs and little aldicarb (I) remains. The signal from the methylthio protons (peaks 7 and 8) does not undergo extensive chemical shift change during the reaction, since these protons are well removed from the reaction site in the molecule.

The signals from the *N*-methyl protons (peak 3 in Figure 3A,B) in aldicarb (I) diminish as the reaction proceeds, and signals at 2.59 ppm (peak 5) and 2.66 ppm (peak 4) appear. Previous mechanism studies of alkaline hydrolysis of carbamate esters have shown that the portion of the ester

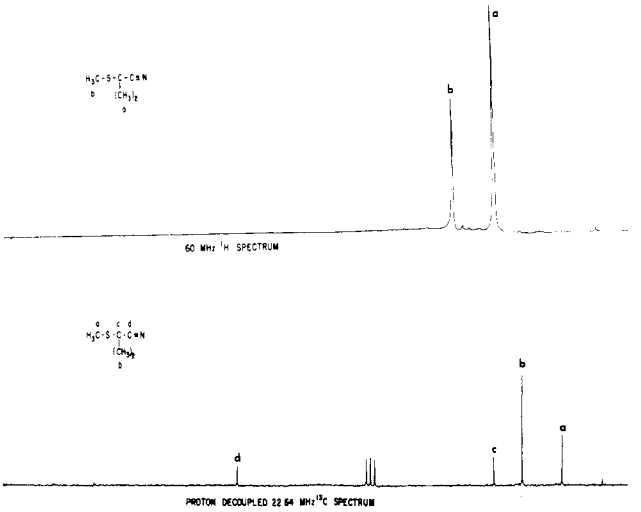

Figure 4. Proton and ^{13}C NMR spectra of aldicarb nitrile (III) [2-methyl-2-(methylthio)propionitrile]. For the proton NMR the labeled assigned peaks are as follows (in ppm): a, 1.65; b, 2.23. For the ^{13}C NMR the labeled assigned peaks are as follows (in ppm); a, 13.64; b, 27.23; c, 36.52; d, 121.66.

containing the *N*-methyl protons cleaves from the molecule, along with the carboxyl group, to form a substituted carbamic acid (Bender and Homer, 1965; Vontor et al., 1972; Dittert and Higuchi, 1963; Christenson, 1964). The hydrolysis mechanism can involve either a tetrahedral ($B_{AC}2$) or isocyanate (El_cB) intermediate in the rate-determining step depending upon the structure of the ester (Wolfe et al., 1978). The carbamic acid formed by either path is rapidly hydrolyzed to methylamine and carbon dioxide. Peak 5 at 2.59 ppm has been identified through addition of small amounts of known material (doping) to be methylamine. Peak 4 at 2.661 ppm was identified through a series of experiments and assigned to 1,3-dimethylurea (vide infra).

Depicted in Figure 3D is the product composition after a reaction time of greater than three half-lives. The major product of the reaction is aldicarb oxime (II) (peaks 2, 8, and 11), which accounts for about 85% of the total product composition. The two signals, 2.32 and 1.654 ppm (1:2 ratio), have been assigned to the minor product of the hydrolysis reaction. This compound has been identified by NMR spectroscopy, GLC, and IR analysis to be 2-methyl-2-(methylthio)propionitrile, III (aldicarb nitrile) (Figure 4). The signal at 2.32 ppm (peak 6) is ascribed to the methylthio protons and peak 9 at 1.654 ppm was assigned to the *gem*-dimethyl proton resonance. The mechanism for the formation of this minor product is discussed later.

Thus, the simplicity of analysis by FT NMR has made this technique extremely useful for analyzing the kinetics of the hydrolysis reaction. A plot of ln percent residual aldicarb (I) vs. time constructed from this data is shown in Figure 5. The pseudo-first-order rate constant obtained from the slope of this line was calculated by using a linear regression analysis.

Further kinetic experiments were done to examine the mechanistic details leading to the major and minor products of hydrolysis. Initially, the concentration of carbamate ester was varied to reflect a rate change if carbamate concentration appeared in the rate equation at an order greater than 1. The plot of log k_{obsd} vs. log concentration was linear with a slope of zero over the concentration range studied (0.005–0.020 M). This result confirms a first-order dependency of the rate of hydrolysis on carbamate ester concentration.

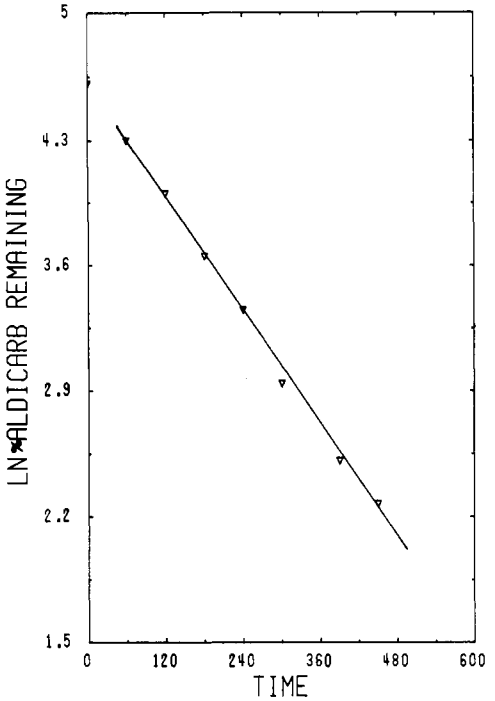

Figure 5. Plot of ln percent aldicarb (I) remaining vs. time in minutes. Reaction in D_2O was studied at 90 °C with phosphate buffer at pD 7.53 and ionic strength maintained at 0.70 M with potassium chloride. Initial aldicarb concentration was 0.0087 M.

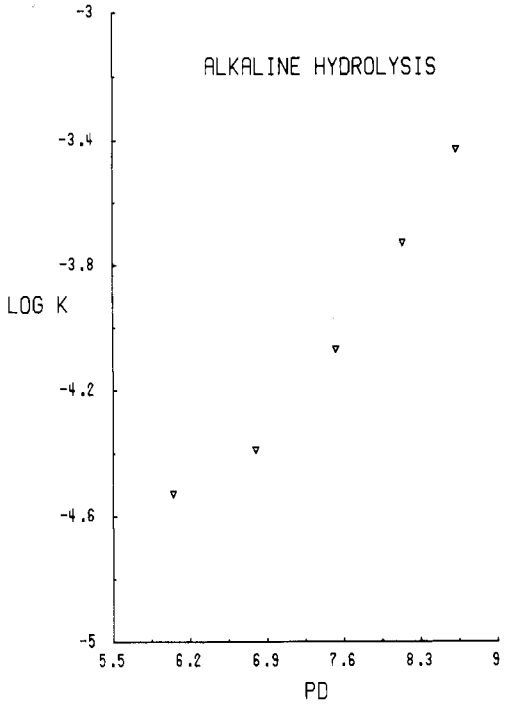

Figure 6. Plot of log k_{obsd} vs. pD for aldicarb (I) hydrolysis using the data in Table II.

Table II. Dependency of the Rate of Aldicarb (I) Hydrolysis on Deuterioxide Concentration[a-c,e]

pD	k_1 ($\times 10^4$), s^{-1}	log k_1
8.63	3.58	
	3.72	
	3.63	
	3.87	
	mean: 3.70	−3.43
8.14	1.91[d]	
	2.10[d]	
	1.87	
	1.87	
	1.37[c]	
	1.48[c]	
	mean: 1.77	−3.75
7.53	0.90	
	0.88	
	0.87	
	mean: 0.89	−4.05
6.80	0.40	
	0.403	
	0.395	
	0.443	
	mean: 0.41	−4.39
6.05	0.31	
	0.31	
	0.30	
	0.31	
	mean: 0.308	−4.51

[a] 0.05 M deuterated phosphate buffers, except as noted for experiments at pD 8.14. Ionic strength raised to 0.70 with potassium chloride. [b] At 90 °C with substrate concentration at 0.0087 M. [c] Analyzed by FT NMR. [d] 0.10 M phopshate buffer with iooic strength raised to 0.70 M with potassium chloride. [e] Duplicate experiments at each pD and temperature were run and average values for the rate constants were calculated from the data for a minimum of two or three measurements and usually more. The precision by this method is ±10%.

The possibility of buffer catalysis in aldicarb hydrolysis was examined by varying buffer molarity over a 10-fold range in concentration. The results, summarized in Table II, demonstrate that buffer catalysis does not represent a major contribution to the rate of the reaction. The observed rate constants are identical within experimental error over a 10-fold increase in buffer concentration. Although there is a slight decrease in kinetic velocity at the lowest buffer concentration, it is far from the expected rate decrease for a 10-fold dilution of buffer strength. Moreover, halving the buffer molarity produces no change in the kinetic velocity and provides added credibility that buffer catalysis is negligible.

The rate dependency of the deuterioxide ion concentration was investigated over a range from pD 6.0 to pD 8.6 in phosphate buffer, and the kinetics were determined by FT NMR as before. Previous literature reports on hydrolysis of carbamate esters summarized by Aly and El-Dib (1971) demonstrated a first-order dependency on base concentration. The experimental results in Table II and Figure 6 demonstrate that at high pD the plot of log rate vs. pD is linear and therefore a dependency of the rate upon the deuterioxide ion concentration. There are, however, two remarkable features. At lower pD, a surprising deviation from linearity is observed. The explanation for this behavior at lower pD is discussed subsequently. An equally unusual observation is that the slope is 0.62 so that the reaction is fractional order in base. This nonintegral dependence while not easily explained has considerable precedence in herbicide hydrolysis studies (Plust et al., 1981) and more recently in the hydrolysis of the insecticide chloropyrifos (Macalady and Wolfe, 1983). Additionally, neither product, temperature, nor isotope studies reveal anomalies. Accordingly, the discrepancy does not appear to raise a serious mechanistic ambiguity.

The Arrhenius activation parameters were determined at pD 7.53 from the pseudo-first-order rate constants for the reaction at various temperatures. The plot of ln (k_{obsd}/T) vs. $1/T$ (Figure 7) is linear over the temperature range studied, and ΔH^* was obtained from the slope of the line. The value of the activation entropy is particularly significant as a diagnostic for the mechanism of hydrolysis. The entropy value, $\Delta S^* = -5.8$ eu, is more positive by some 20 eu than that typical of carbamates that hydrolyze by the $B_{AC}2$ mechanism involving a tetrahedral intermediate (Christenson, 1964). On the other hand, this entropy value

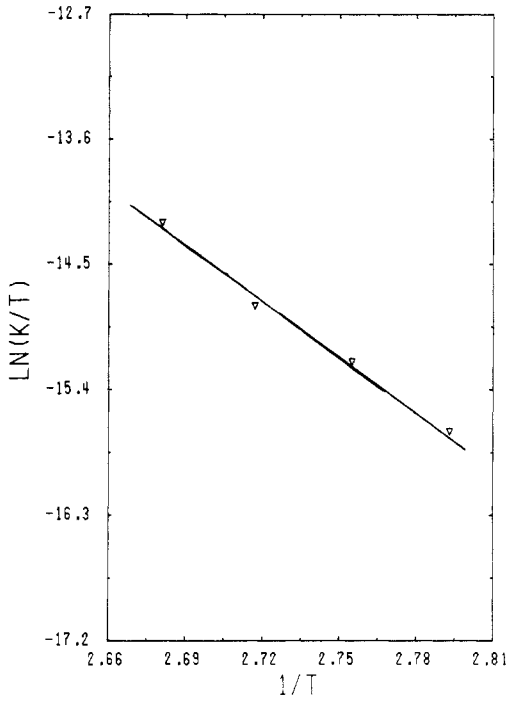

Figure 7. Plot of ln (k_{obs}/T) vs. $1/T$ for hydrolysis of aldicarb (I) at pD 7.53.

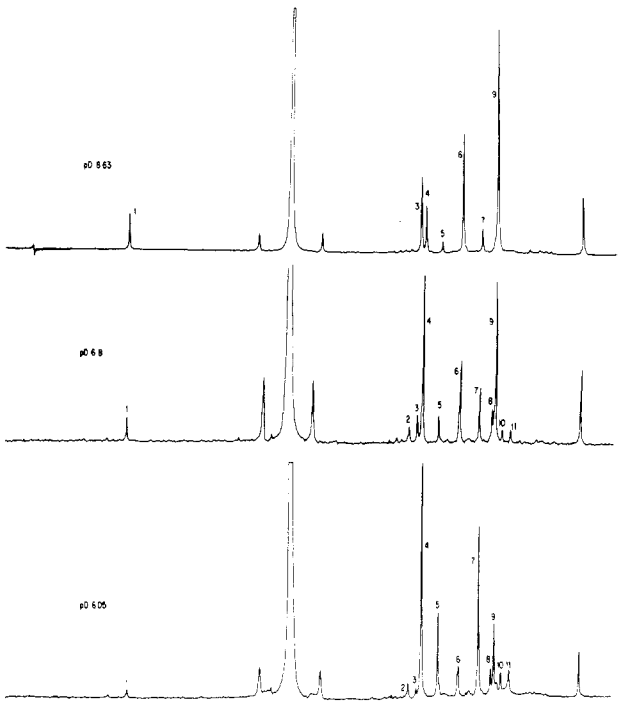

Figure 8. 90-MHz proton NMR spectra for aldicarb hydrolysis in deuterated phosphate buffers at varying pD values.

Scheme I. Proposed Mechanism of Hydrolysis for Aldicarb (I) in Alkaline Media

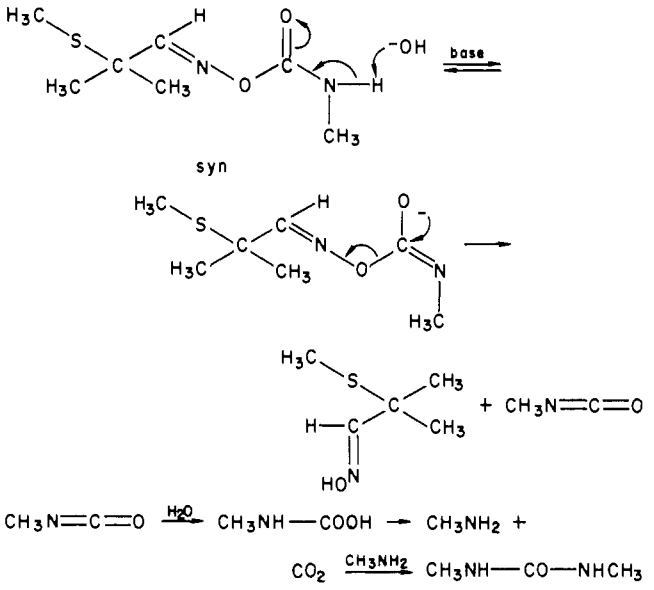

is consistent with entropy values obtained for other carbamate esters that hydrolyze by the El_cB elimination–addition pathway involving an isocyanate intermediate in the rate-determining step (Bender and Homer, 1965; Christenson, 1964).

These results and the following additional experiments proved to be definitive in determining the mechanism shown in Scheme I. The presence of the isocyanate intermediate formed during an El_cB reaction was demonstrated by intermolecular trapping of the isocyanate with an appropriate nucleophile. The high reactivity of isocyanates toward amines is well established (Hegarty and Frost, 1973; Williams and Jencks, 1974). Amine trapping of the intermediate isocyanate readily afforded a substituted urea, namely, 1,3-dimethylurea identified by NMR, IR, and melting point.

Additional evidence for this mechanism was provided by isotope studies when the alkaline hydrolysis was followed at equal deuterium oxide ion concentration in both aqueous (HPLC) and deuterated (FT NMR) buffers. An inverse deuterium oxide kinetic isotope effect was observed (k_D/k_H = 2.47) (Eadon and Chi-Tsiu, 1982). This is consistent with a rapid preequilibrium formation of the anion followed by decomposition of the anion in the rate-determining step. There is also an inverse deuterium oxide kinetic isotope effect of similar magnitude (k_D/k_H = 1.8) in the *p*-nitrophenyl *N*-methylcarbamate hydrolysis by the El_cB mechanism (Bender and Homer, 1965).

The previous discussions provide convincing evidence that the hydrolysis of aldicarb (I) proceeds by an El_cB mechanism with the formation of an isocyanate intermediate and lead to the mechanism presented in Scheme I as the pathway for alkaline hydrolysis of aldicarb (I). The entropy of activation for alkaline hydrolysis is 20 eu more positive compared to that of esters hydrolyzing by the $B_{AC}2$ mechanism. The observance of urea formation is indicative of the presence of the isocyanate intermediate and is characteristic of the El_cB reaction pathway. Additionally, no buffer catalysis was observed as the molarity of the buffer was increased 10-fold for aldicarb hydrolysis. Finally, the presence of an inverse deuterium oxide kinetic isotope effect is evidence of a rapid preequilibrium formation of the anion followed by a slow, rate-determining decomposition to form the isocyanate intermediate.

Whereas the dependency of the rate of hydrolysis upon the deuterioxide ion concentration was linear at high pD, there was a marked deviation from linearity at lower pD value (Figure 6). This change in rate was accompanied by a change in the product composition as the acidity increased. NMR spectra of the reaction composition at varying pD (Figure 8) illustrate this change. Figure 8A is the end product composition for the hydrolysis at pD 8.63. The major product of the reaction is the expected aldicarb oxime (II) (peaks 1, 6, and 9), which accounts for nearly 90% of the reaction composition. Peaks 3 and 4 are ascribed to the products of methyl isocyanate hydrolysis, namely, 1,3-dimethylurea and methylamine, respectively.

Table III. Pseudo-First-Order Rate Constants for the Acid-Catalyzed Hydrolysis of Aldicarb (I) at 90 °C[a-c]

pD	k_1 ($\times 10^5$) s^{-1}	log k_1
3.0	21.0	
	19.5	
	23.2	
	21.3	
	mean: 21.3	−3.67
3.6	13.0	
	12.5	
	12.8	
	mean: 12.8	−3.89
4.0	6.7	
	6.87	
	6.84	
	mean: 6.82	−4.17
4.8	2.8	
	2.9	
	mean: 2.85	−4.55
5.0	2.54	
	2.61	
	2.56	
	2.51	
	mean: 2.56	−4.59
5.6	2.42	
	2.45	
	mean: 2.44	−4.61

[a] 0.05 M deuterated citrate/phosphate buffers with ionic strength raised to 0.70 with potassium chloride. Initial aldicarb (I) concentrations 0.0087 M. [b] Analyzed by FT NMR. [c] Duplicate experiments at each pD and temperature were run and average values for the rate constants were calculated from the data for a minimum of two or three measurements and usually more. The precision by this method is ±10%.

The small signals (peaks 5 and 7) are due to aldicarb nitrile (III) and account for the remaining 10% of the final reaction composition at this pD.

Significant changes are found in the product composition from reaction run at pD 6.8 (Figure 8B). Apart from the residual aldicarb (I) (peaks 2 and 8), the complexity of the spectrum has increased considerably. Several components in the spectrum have increased in intensity at the expense of others. Peak 4, ascribed to methylamine, is now very large compared to the 1,3-dimethylurea signal (peak 3). This change in the product composition reflects the change in methylisocyanate hydrolysis with increasing acidity. The hydrolysis of methyl isocyanate leading to methylamine and CO_2 (Tiger et al., 1971) is accelerated in the presence of increased concentrations of $HClO_4$. The decomposition of the carbamate ion, initially formed in the hydrolysis of the methyl isocyanate, is also acid catalyzed (Johnson and Morrison, 1972; Caplow, 1968), and the products of this reaction are methylammonium ion and carbon dioxide. In acidic media the amine is largely protonated and has greatly reduced reactivity for methyl isocyanate, thus reducing or ceasing urea formation. The signal for methylamine (2.59 ppm) is enhanced at the expense of the urea resonance at 2.661 ppm.

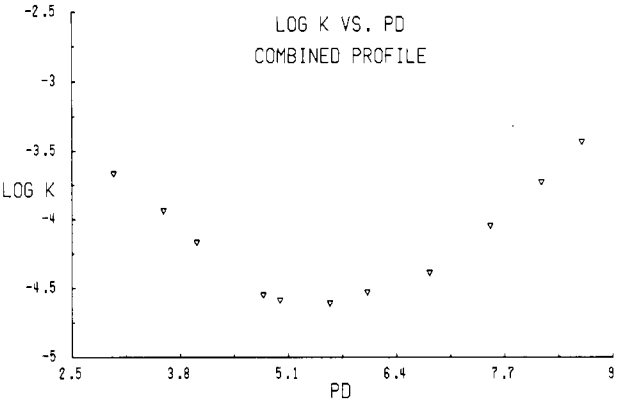

Figure 9. Plot of log k_{obsd} vs. pD for aldicarb (I) hydrolysis from pD 3.0 to 8.63 using the data of Tables II and III.

Figure 8C illustrates the product composition at pD 6.05. The spectrum is similar to Figure 8B in products; however, the ratio of these products has changed dramatically. Most importantly, aldicarb nitrile (III) (peaks 5 and 7) is now the major product of the reaction comprising over 50% of the total product composition. Aldicarb oxime (II) is a minor contributor at 30% of the total. Finally, there are two singlets at 1.288 and 1.15 ppm (peaks 10 and 11) that are assigned to the carbinolamine (V) of aldicarb oxime (II) and contribute about 20% of the product composition. In summary, these changes in kinetics and product composition indicate a change in reaction mechanism and/or the presence of a competing reaction. This proved to be an acid-catalyzed reaction as shown in Scheme II.

To evaluate this component, the hydrolysis was followed in a series of deuterated citrate/phosphate buffers varying in acidity from pD 3.0 to 5.6. The pseudo-first-order rate constants are recorded in Table III. The kinetics have a fractional order (0.5) dependency on hydronium ion concentration as indicated from the linear portion of the plot of log k_{obsd} vs. pD (below pD 5.0) in Figure 9. Here as in the base-catalyzed reaction and in direct analogy with herbicide hydrolysis (Plust et al., 1981), unusual fractional order dependencies are observed. As expected, a deviation from linearity is observed in the region pD 5.0–6.0 corresponding to the pD where the reaction is subject to both acid and basic catalysis. Combining the kinetic data for both the acidic and alkaline hydrolyses in the region pD 3.0–8.6, we obtained a pD–rate profile (log k_{obsd} vs. pD; Figure 9) that illustrates the competing pathways for aldicarb hydrolysis as a U-shaped curve. This combined curve displays a region where the reaction is a function of

Table IV. Product Composition (Percent) for the Hydrolysis of Aldicarb (I) in 0.05 M Citrate/Phosphate (Acidic pD) or Phosphate Buffers (Alkaline pD) at Various pD Values[a]

pD	oxime (II)	nitrile (III)	aldehyde (IV)	carbinolamine (V)	DMU[b,d]	MA[c,d]
3.0		78	22			
3.6		78	22			
4.0		78	22			
4.8		70	11	20		
5.0		69	9	24		100
5.6	13	54	11	22		100
6.05	28	51		20		100
6.8	66	19		15	8	92
7.53	78	13		8	16	84
8.14	85	15			24	76
8.63	89	11			42	58

[a] Detection by FT NMR. [b] DMU = 1,3-dimethylurea. [c] MA = methylamine. [d] The products resulting from hydrolysis of methyl isocyanate (DMU, MA) were calculated as a separate reaction.

Scheme II. A Mechanism for Hydrolysis of Aldicarb (I) in Acidic Media (Syn Configuration)

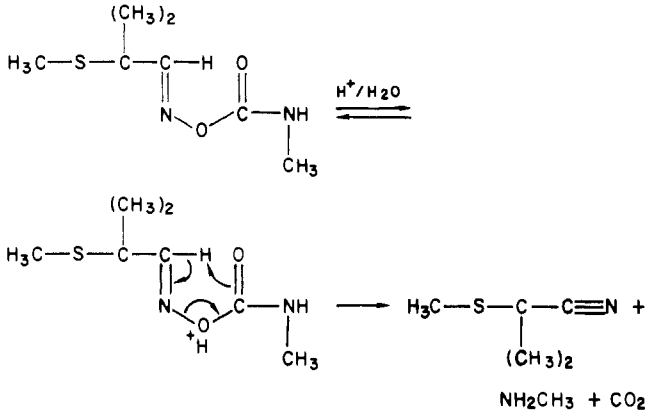

deuterioxide concentration leading to the oxime (II) as the major product, a region where the reaction is a function of deuterium ion concentration leading to the nitrile (III) as the major product, and a region near neutrality where the reaction is subject to both mechanisms.

Table IV summarizes the product composition for aldicarb hydrolysis in citrate/phosphate (acidic pD) or phosphate (alkaline pD) buffers at various pD values. Inspection of Table IV reveals the complex changes in product composition that accompany the observed changes in mechanism. Importantly, it exemplifies the uniqueness and complexity of aldicarb hydrolysis compared to many other carbamate esters that have only an alkaline pathway leading to a single set of products. Further, the region near neutrality, where the reaction is most complex and the rate the slowest, is the pH typical of most natural water systems.

A mechanism that accounts for the observed kinetics and the formation of aldicarb nitrile (III) as the major product during acidic hydrolysis is presented in Scheme II. The oxygen is protonated and then in a six-membered transition state there is a 1,2-elimination to form the nitrile (III) and the substituted carbamic acid. There is a large decrease in steric strain in going from the oxime ester to the nitrile, and this may provide some driving force. Finally, the carbamic acid readily hydrolyzes by an acid-catalyzed reaction to form methylamine and CO_2.

Discussion of the proposed mechanisms for hydrolysis of aldicarb (I) in both alkaline and acidic media has thus far accounted only for the formation of the major products of the reaction. Attention is now directed to account for formation of the minor products of each reaction. For the alkaline reaction, aldicarb nitrile (III) accounts for 11% of the product composition at pD 8.63, whereas, for the acidic reaction, the aldehyde (IV), which arises from acidic decomposition of aldicarb oxime (II) via the carbonolamine (V), accounts for 22% of the product composition at pD 3.0. Closer examination of the rates of the formation of these minor compounds provides evidence for rationalizing these results.

Kinetic data for nitrile (III) formation in the alkaline hydrolysis of aldicarb (I) was analyzed. The log plot (see legend, Figure 10) displays a curve with two distinct slopes, suggesting a change in reaction mechanism. As indicated, the rate of initial nitrile (III) formation is rapid and approximately 4 times faster than the rate of aldicarb hydrolysis; this accounts for about 6% of the total product composition for the reaction. After this initial formation, nitrile (III) is produced more slowly at a rate approximately 4 times slower than the rate of aldicarb (I) hydrolysis.

An explanation consistent with these data is that initial

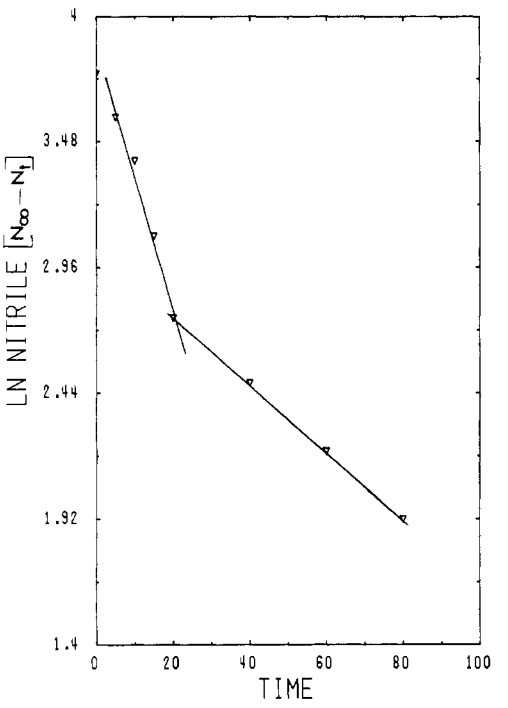

Figure 10. Plot of nitrile (III) formation (nitrile at $t = \infty$–nitrile at t) vs. time in minutes for hydrolysis of aldicarb (I) at pD 8.63.

rapid nitrile(III) production results from alkaline hydrolysis of the anti isomer of aldicarb (I) (eq 1).

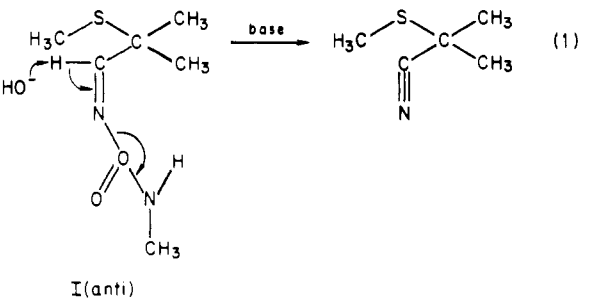

(1)

The correspondence between the amount of this isomer and the product is good, and the geometry for this kind of reaction is ideal (Hauser and Jordan, 1936). The formation of the remaining nitrile(III) is consistent with the El_cB mechanism and the observed kinetics for *syn*-aldicarb hydrolysis. Following the preequilibrium formation of the anion, a second reaction (eq 2) can compete with the slow

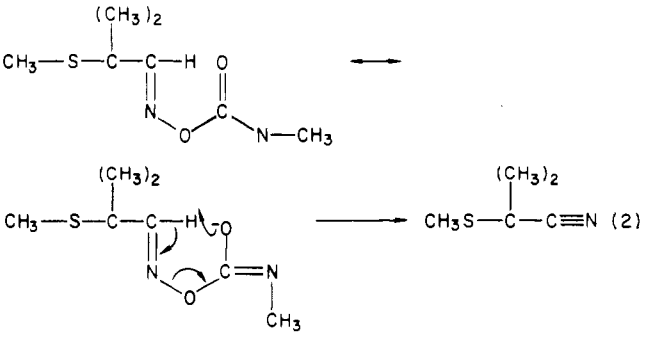

(2)

isocyanate formation leading to nitrile (III). Since nitrile formation requires a special orientation of the molecule for proton abstraction, the rate is expected to be slower and thus yields the remaining 5% of the product.

Additional supporting evidence for this explanation is that as the temperature increases, at constant pD, the

amount of nitrile (III) formed by eq 2 decreases. This is likely because the rate of acyl–oxygen fission is accelerated by a temperature increase, whereas the reaction (eq 2) would be more favorable at lower temperature due to the entropy considerations involved in achieving the proper orientation. When plotted, there is a linear decrease in nitrile (III) as the temperature of the reaction is increased. Approximately a 2.5% increase in nitrile (III) is produced for every 10 deg decrease in temperature. With this mechanism, a plausible explanation for all of the products and kinetics of the alkaline hydrolysis of aldicarb (I) is provided.

A related rationale may be used to account for the production of the substantial amounts of aldehyde (IV) (Table IV) produced during the acidic hydrolysis of aldicarb (I). The aldehyde (IV) is produced in the reaction of aldicarb oxime (II) in acidic media. In separate experiments, aldicarb oxime (II) was converted initially to the carbinolaminine (V) and then to the aldehyde (IV) in acidic media. Equation 3 depicts a mechanism for formation of oxime from the anti isomer of aldicarb in acid. Obtaining a rate for the formation of the oxime from the anti isomer was impossible due to complications from conversion of the oxime to aldehyde (IV) via the carbinolamine intermediate (V). Nevertheless, in analogy with the base-catalyzed reaction, approximately 6% of the oxime can be assumed to arise from the reaction of the anti isomer. The remainder of the oxime (aldehyde) formed likely arises from another mechanism operating with the syn isomer of aldicarb. Presumably this could take place by attack of water upon the C=N double bond of aldicarb leading to a carbinolamine intermediate, which breaks down (eq 3) to the aldehyde (IV). The relatively large quantities of aldehyde (eq 3) formed (22%) indicate that an alternate reaction pathway, perhaps one involving attack by water at the C=N double bond, is reasonably efficient. This type of reaction mechanism has precedence (Cordes and Jencks, 1963) and serves as a rationale to account for the amounts and products observed in the reaction.

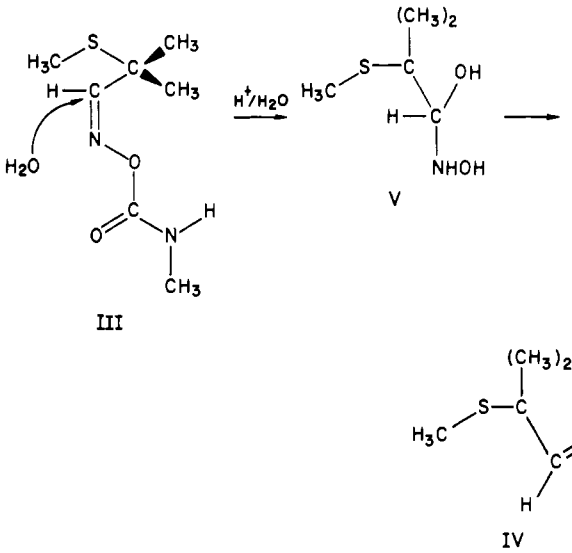

CONCLUSION

This investigation provides rates, product composition, and reaction mechanisms for the hydrolysis of syn and anti isomers of aldicarb (I) in both alkaline and acidic media. The kinetic data and proposed mechanisms for alkaline hydrolysis are consistent with reports on a wide variety of carbamates. However, the acid-catalyzed reaction, which competes with alkaline hydrolysis at neutral pH and dominates in acidic media, is unique to this aldoxime carbamate. This is likely due to, among other things, the large steric strain of the 2-(methylthio)propyl group that drives the reaction toward steric relief and the production of the nitrile.

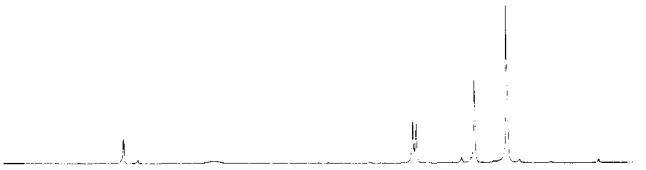

Figure 11. Proton NMR of aldicarb (I) after 300 days at 6 °C in pD 5.0 citrate/phosphate buffer. Sample stored in the dark shows no measurable hydrolysis.

The investigation also revealed that the minor products formed during the reaction arise from a combination of reactions occurring on the anti isomer of aldicarb (I), as well as an alternative reaction mechanism operating on the syn isomer. Nitrile production during alkaline hydrolysis was derived from two distinct reactions: an initial rapid formation, accounting for approximately 7% of the total nitrile produced resulting from hydrolysis of the anti isomer, and a slower reaction (eq 2), accounting for the remainder.

Of interest to environmental extrapolations is the temperature dependence of nitrile formation during alkaline hydrolysis. At constant pH, approximately a 2.5% increase in nitrile formation is observed for every 10-deg decrease in temperature. If it is assumed that this pattern continues, as much as 33% nitrile could be produced at 11 °C. Importantly, if the mechanism presented in eq 4 is operative at pH 5.6 and 11 °C, more nitrile may be produced than the data at the higher temperatures suggest. However, since in this region the reaction rate is the slowest and the product composition the most complex (Table IV), accurate prediction of the contribution of this reaction pathway under these circumstances is impossible.

A preliminary investigation of the toxicity of the products of the reaction indicate that they probably do not present a serious health hazzard, as their toxicities have been reported to be relatively low (Spurs and Sousa, 1974). However, the rate of decomposition of aldicarb (I), at the temperature and pH of the Long Island aquifer, was found to be very slow. When extrapolated to the temperature of 11 °C, the half-life of aldicarb (I) decomposition was found to be 5.8 years (Figure 11). At the levels of contamination originally found in the wells, in the absence of the usually important oxidative pathways, at least six half-lives would be required to decrease the level of aldicarb (I) in the water from the current value of about 400 ppb to the allowable limit of 7 ppb (Guerrera, 1981). Aldicarb (I), or any other similar caramate contaminant entering the aquifer, will be stable to decomposition and likely remain a contaminant for many years.

ACKNOWLEDGMENT

We acknowledge with gratitude helpful discussions with Dr. George Eadon of the New York State Health Laboratories.

Registry No. I, 116-06-3; II, 1646-75-9; III, 10074-86-9; IV, 16042-21-0; 1,3-dimethylurea, 96-31-1; methylamine, 74-89-5; 2-methylpropene nitrosochloride dimer, 24993-16-6; carbon dioxide, 124-38-9.

LITERATURE CITED

Aly, O. A.; El-Dib, M. A. *Water Res.* **1971**, *5*, 1191
Bender, M. L.; Homer, R. B., *J. Org. Chem.* **1965**, *30*, 3975.
Caplow, M. *J. Am. Chem. Soc.* **1968**, *90*, 6795.

Christenson, I. *Acta Chem. Scand.* **1964**, *18*, 904.
Cohen, S. Z.; Creeger, S. M.; Carsel, R. F.; Infield, C. G. *ACS Symp. Ser.* **1984**, in press.
Cordes, E. H.; Jencks, W. P. *J. Am. Chem. Soc.* **1963**, *85*, 2843.
Dittert, L. W.; Higuchi, G. *J. Pharm. Sci.* **1963**, *52*, 852.
Eadon, G., New York State Health Laboratories, unpublished work, 1984.
Eadon, G.; Chi-Tsiu, New York State Health Laboratories, unpublished work, 1982.
Emerson, W. S. *J. Am. Chem. Soc.* **1951**, *73*, 1854.
Fieser, L. F.; Fieser, M. "Reagents for Organic Syntheses"; Wiley: New York, 1967; Vol. I, p 1065.
Glasoe, P. K.; Long, F. A. *J. Phys. Chem.* **1960**, *64*, 188.
Gomori, G. *Methods enzymol.* **1955**, *1*, 138.
Guerrera, A. A. *J—Am. Water Works Assoc.* **1981**, *73*, 190.
Hansen, J. L.; Spiegel, M. H. *Environ. Toxicol. Chem.* **1983**, *2*, 147.
Hauser, C. R.; Jordon, E. *J. Am. Chem. Soc.* **1935**, *57*, 2450.
Hauser C. R.; Jordon, E. *J. Am. Chem. Soc.* **1936**, *58*, 1777.
Hegarty, A. F.; Frost, L. *J. Chem. Soc., Perkins Trans. 2* **1973**, 1719.
Johnson, S. L.; Morrison, D. L. *J. Am. Chem. Soc.* **1972**, *94*, 1323.
Macalady, D. L.; Wolfe, N. L. *J. Agric. Food Chem.* **1983**, *31*, 1139.
Macomber, R. S. *J. Am. Chem. Soc.* **1983**, *105*, 4386.
Maitlen, J. C.; Powell, D. M. *J. Agric. Food Chem.* **1982**, *30*, 589.
Meinwald, J.; Meinwald, Y. C.; Baker, T. N., III *J. Am. Chem. Soc.* **1964**, *86*, 4074.
Okuyama, T.; Fueno, T. *J. Am. Chem. Soc.* **1983**, *105*, 4390.
Payne, L. K., Jr.; Stanbury, H. A., Jr.; Weiden, M. H. J. *J. Agric. Food Chem.* **1966**, *14*, 356.
Plust, S. J.; Loehe, J. R.; Feher, F. J.; Benedict, J. H.; Herbrandson, H. F. *J. Org. Chem.* **1981**, *46*, 36561.
Richey, F. A., Jr.; Bartley, W. J.; Sheets, K. P. *J. Agric. Food Chem.* **1977**, *25*, 47.
Spurs, H. W., Jr.; Sousa, A. A. *J. Environ. Qual.* **1974**, *3*, 130.
Tiger, R. P.; Behhli, L. S.; Entilis, S. G. *Kinet. Katal. (Engl. Transl.)* **1971**, *12*, 318.
Vontor, T.; Cosha, J.; Vecera, M. *Collect. Czech. Chem. Commun.* **1972**, *27*, 2183.
Weiden, M. H. J.; Moorefield, H. H.; Payne, C. K. *J. Econ Entomol.* **1965**, *58*, 154.
Williams, A.; Jencks, W. P. *J. Chem. Soc., Perkin Trans. 2* **1974**, 1753.
Wolfe, N. L.; Zepp, R. G.; Paris, D. F. *Water Res.* **1978**, *12*, 561.

Received for review January 30, 1984. Revised manuscript received May 14, 1984. Accepted August 9, 1984. Presented at the 13th Northeastern Regional Meeting, American Chemical Society, Hartford, CT, June 29, 1983.

Dermal Exposure to Carbaryl by Strawberry Harvesters

Gunter Zweig,*[1] Ru-yu Gao,[2] James M. Witt,[3] William Popendorf,[4] and Kenneth Bogen

Dermal exposure to carbaryl by 18 strawberry harvesters was measured in the morning and afternoon on three consecutive days. Pesticide exposure was estimated from cotton gauze patches and light cotton gloves worn by the workers throughout the workday or shorter time periods. Carbaryl concentrations were determined on patches, gloves, and strawberry plants by reverse-phase high-performance liquid chromatography (HPLC). The study has revealed that during the early morning period, when there was a considerable dew deposited on leaves, carbaryl exposure was usually higher than in the afternoon. Classification of pickers by age and body weight showed that younger and/or lighter subjects exhibited lower dermal carbaryl exposure, expressed as dose rate (mg/h). The ratios of dermal exposure to dislodgeable foliar residues were within the same order of magnitude as those obtained from other pesticide–crop experiments found in the literature.

Studies on the assessment of pesticide exposure (captan and benomyl) by strawberry harvesters have been reported by Popendorf et al. (1982), Everhart and Holt (1982), Zweig et al. (1983), and, most recently, Winterlin et al. (1984). In an effort to examine possible differences in pesticide exposure by different age groups of harvesters, this study reported here was designed to examine the exposure to the insecticide carbaryl (1-naphthyl *N*-methylcarbamate) by a group of strawberry harvesters, ranging in ages from 12 to 40. These results were to be compared with those from

Table I. Physical Characteristics and Productivity of Strawberry Harvesters

ID	sex	age	wt, kg	ht, cm	surface area, m^2	daily prod. crates/h
6	F	40	69.5	168	1.77	1.04
7	F	12	42.3	163	1.52	0.68
8	F	18	63.6	175	1.78	0.91
9	F	29	56.7	164	1.58	0.99
10	F	13	43.1	149	1.35	0.78
11	F	32	61.3	175	1.72	1.00
12	F	15	59.0	160	1.62	1.00
13	F	16	50.4	173	1.56	0.72
14	M	13	63.6	178	1.76	0.97
15	M	13	70.4	168	1.78	0.57
17	F	12	45.4	157	1.42	0.74
18	F	12	49.9	163	1.52	0.60
20	M	14	56.7	180	1.70	1.04
21	F	14	54.5	165	1.59	0.60
22	F	37	49.9	152	1.46	0.89
23	F	16	49.9	165	1.53	0.96
25	M	12	45.4	160	1.43	0.70
26	M	15	63.6	183	1.84	0.72

Pesticide Hazard Assessment Program (PHAP), University of California, School of Public Health, and Sanitary Engineering and Environmental Health Research Laboratory, Richmond Field Station, Richmond, California 94804.
[1] Present address: Office of Pesticide Programs, Environmental Protection Agency, Washington, DC 20460.
[2] Present address: Nankai University, Tianjin, People's Republic of China.
[3] Present address: Oregon State University, Corvallis, OR.
[4] Present address: Institute for Agricultural Medicine, University of Iowa, Iowa City, IA.

0021-8561/84/1432-1232$01.50/0